

**The Microwave Spectrum and Molecular Structure of Vinyl Chloride-Acetylene, A Side-
Binding Complex**

Helen O. Leung*, Mark D. Marshall*, and Fan Feng

Department of Chemistry, Amherst College, P.O. Box 5000, Amherst, MA 01002-5000

Address for correspondence: Prof. Mark D. Marshall
Department of Chemistry
Amherst College
P.O. Box 5000
Amherst, MA 01002-5000
Telephone: +01 413-542-2006
Fax: +01 413-542-2735
E-mail: mdmarshall@amherst.edu

*To whom correspondence should be addressed. Tel: +01 413-542-2006; E-mail:

mdmarshall@amherst.edu (MDM); Tel: +01 413-542-2660; E-mail: hleung@amherst.edu

(HOL); Fax: +01 413-542-2735

The authors declare no competing financial interest.

Abstract:

The structure of the gas-phase bimolecular complex formed between vinyl chloride and acetylene is determined using a combination of broadband, chirped-pulse and narrow band, Balle-Flygare Fourier transform microwave spectroscopy from 5.8 to 20.7 GHz. Although all previous examples of complexes formed between protic acids and haloethylenes are observed to have similar modes of binding regardless of the specific identity of the acid, HF, HCl, or HCCH, the vinyl chloride-HCCH complex has HCCH located at one end of the vinyl chloride with the secondary interaction occurring with the geminal hydrogen atom as opposed to the “top” binding configuration found for vinyl chloride-HF. Nevertheless, the details of the structure, such as hydrogen bond length (3.01 Å) and amount of deviation from linearity (58.5°), do reflect the strength of the interaction and show clear correlations with the gas-phase acidity. Comparison with analogous complexes allows the determination of the relative importance of electrostatic interactions and steric requirements in leading to the observed structures.

Keywords: intermolecular interactions, nuclear quadrupole coupling, chirped pulse, steric requirements, electrostatics

1. Introduction

By modifying the electron density of ethylene through an increase in the number of fluorine substituents, a systematic change in the nature of its interaction with a protic acid HX (HX = HF,¹⁻³ HCl,^{2,4-7} and HCCH⁸⁻¹⁰) has been observed through work in our group and in the Legon group. The fluoroethylene-HX complexes are effectively planar, each with two interactions: a primary hydrogen bond between the acid and an F atom in the ethylene subunit and a secondary interaction, made possible by a bend in the hydrogen bond, between the nucleophilic portion of the acid and an H atom in the ethylene subunit. These interactions occur across the C=C bond for vinyl fluoride and 1,1-difluoroethylene (“top” binding configuration, Fig. 1a) but lie at one end of the C=C bond for 1,1,2-trifluoroethylene (“side” binding configuration, Fig. 1b). The different motifs provide valuable information regarding the compromise between electrostatic and steric factors, and the contribution of the latter to the structures of these complexes has been discerned through a study of *trans*-1,2-difluoroethylene-HF.¹¹ Because the two F atoms and the two H atoms in *trans*-1,2-difluoroethylene form electrostatically equivalent pairs, the preference for HF to bind across the C=C double bond indicates that this configuration is sterically more favorable.

For vinyl fluoride, the hydrogen atoms are not electrostatically equivalent. In fact, because of its proximity to the F atom, the geminal H atom is expected to be more electropositive than the H atom located *cis* to the F atom. Thus, the side configuration should have greater electrostatic stability. The observed top binding configuration, therefore, is driven by steric factors. On the other hand, since 1,1,2-trifluoroethylene complexes assume a sterically unfavorable side binding configuration, it follows then that the binding mode must be driven by electrostatic factors. Indeed, mapping the electrostatic potential of 1,1,2-trifluoroethylene onto

its total electron density shows that the F atom geminal to the H atom (that is, the F atom that participates in the hydrogen bond with the acid) is the most negative of the three F atoms. Lastly, because there is no H geminal to an F atom in 1,1-difluoroethylene, only the top binding configuration is observed for its HX complexes. Through studies of the vinyl fluoride, 1,1-difluoroethylene, and 1,1,2-trifluoroethylene complexes, it is notable that the binding motif for the three different acids (HF, HCl, and HCCH) remains unchanged for the same fluoroethylene subunit. Furthermore, for the top binding mode, the CF...H angle is approximately 120° (this angle is fixed for the structural analysis for some complexes), but decreases to 104 – 110° for the side binding configuration.

In addition to the binding motif, details of the strengths of the interactions are reflected through the intermolecular bond lengths and the extent to which the hydrogen bond deviates from linearity. Table 1 summarizes the geometric parameters for 9 complexes. In general, for the same acid partner, as the number of fluorine substituents increases, the hydrogen bond becomes longer and bends more from linearity, indicating that the hydrogen-bonded fluorine atom becomes less nucleophilic. The same general phenomenon regarding the hydrogen bond is observed as the gas-phase acid strength decreases from HF to HCl to HCCH for the same fluoroethylene partner. Indeed, for complexes with both low fluorine nucleophilicity and acid strength the primary interaction length becomes so long that the appropriateness of calling it a hydrogen bond becomes questionable. Nevertheless, the term still serves as a useful label for distinguishing between the CF...H (or CCl...H) and the secondary, as defined above, interactions, and we will use it as such.

Building on what we have learned from fluoroethylene complexes, we have begun an examination of chloroethylene complexes to investigate how Cl, which is less electronegative

but more polarizable than F, affects the nature of intermolecular interaction. We have studied the complex between the simplest chloroethylene, vinyl chloride, and HF.¹² It is planar with a top binding configuration (Fig. 2a) similar to its vinyl fluoride counterpart (Fig. 2b). However, the CCl...H angle is 102.4°, significantly smaller than the corresponding CF...H angle of 121.4°, suggesting that the distribution of the electron densities surrounding the halogen atoms are very different in the two complexes. The small CCl...H angle allows the hydrogen bond in vinyl chloride-HF, while having a deviation from linearity similar to that in vinyl fluoride-HF [19.8(3)° and 19(2)°, respectively], to achieve a shorter secondary interaction of 2.59(1) Å (vs 2.73 Å for vinyl fluoride-HF).

We report here the structure of a second vinyl chloride complex: vinyl chloride-HCCH. Our goals are to further our understanding of the different behaviors of Cl and F in intermolecular interactions, investigate how the change from HF to a weaker acid affects the intermolecular interactions, and whether the trends observed in the fluoroethylene-HX complexes are followed in vinyl chloride-HX.

2. *Ab initio* calculations

To provide a guide in the search for and analysis of the microwave spectrum of vinyl chloride-HCCH, we use GAUSSIAN 09¹³ at the MP2/6-311++ G (2d, 2p) level to explore the interaction potential of the two subunits. Assuming the complex to be planar, as is the case for all fluoroethylene-HX complexes characterized to date and as well as for vinyl chloride-HF, only three geometric parameters, shown in the inset to Fig. 3, are necessary to characterize the complex: R is the distance between the centers of the C=C bond of vinyl chloride and the C≡C bond of acetylene, and θ_{vc} and θ_{HCCH} describe the angular orientations of the vinyl chloride and HCCH subunits, respectively. Restricting the structures of the subunits to be the same as those

for the free monomers,^{14,15} the value of θ_{vc} is varied from 5° to 355° in 10° steps with the values of R and θ_{HCCH} optimized at each step, and the resulting minimum energy path is displayed in Fig. 3. There are two minima that are of importance, and the structures corresponding to these are optimized for all three geometric parameters, R , θ_{vc} and θ_{HCCH} . These structures are displayed in Fig. 4 with chemically relevant interaction lengths and angles labeled. The structure 152 cm^{-1} above the global minimum has a top binding configuration, similar to that of vinyl chloride-HF. In particular, the values of the CCl...H angle, 102° , are the same. This is, however, not the lowest-energy structure of vinyl chloride-HCCH, which is unexpected given that HF and HCCH were previously observed to bind in the same way in their respective fluoroethylene complexes. Instead for vinyl chloride-HCCH, the global minimum corresponds to a structure with HCCH binding to the side of vinyl chloride. A comparison of the two isomers shows that the hydrogen bond in the side binding configuration is longer by 0.0479 \AA and bends by 21.49° more from linearity than that in the top binding configuration, suggesting that it is a weaker bond. On the other hand, the side binding configuration shows a H...acetylenic bond interaction length of 2.8339 \AA , which is 0.1558 \AA shorter than that in the top binding configuration. Thus, this latter interaction is the one that provides the stability for the side binding isomer. There is one additional difference between the two isomers: the value of the CCl...H angle in the side configuration is 15.61° smaller. The predicted rotational constants for each isomer are listed below its structure in Fig. 4.

3. Experiment

A mixture of 1% vinyl chloride and 1% HCCH in Ar at a stagnation pressure of 2 atm is expanded through a 0.8 mm diameter pulsed nozzle to generate the complex. We initially obtained the spectrum in the 6.1 – 18.1 GHz region using a broadband chirped pulse Fourier

transform microwave spectrometer. The transitions for the $\text{CH}_2\text{CH}^{35}\text{Cl}-\text{HCCH}$ and $\text{CH}_2\text{CH}^{37}\text{Cl}-\text{HCCH}$ complexes are readily identified and assigned, and then re-measured at higher resolution using a narrow band Balle-Flygare cavity Fourier transform spectrometer. Additional, weaker transitions due to these two isotopologues that are not observed in the chirped pulse spectrum are measured, as well as transitions for four isotopologues containing a naturally occurring, single substitution in ^{13}C . With the use of isotopically enriched samples of $\text{H}^{13}\text{C}^{13}\text{CH}$ and HCCD , we also obtain the spectra for four more isotopologues, $\text{CH}_2\text{CH}^{35}\text{Cl}-\text{H}^{13}\text{C}^{13}\text{CH}$, $\text{CH}_2\text{CH}^{37}\text{Cl}-\text{H}^{13}\text{C}^{13}\text{CH}$, $\text{CH}_2\text{CH}^{35}\text{Cl}-\text{DCCH}$, and $\text{CH}_2\text{CH}^{37}\text{Cl}-\text{DCCH}$.

The chirped pulse spectrometer has been previously described.^{16,17} Spectra are obtained as a series of 1 GHz bandwidth portions. The chirped pulse duration is 4 μs with 25 W of power, and the free induction decay (FID) is digitized directly at 50 Gs s^{-1} for 10 μs beginning 0.5 μs after the end of the chirped excitation pulse. 10 FIDs are collected during each 500 μs opening of the pulsed gas valve, which operates at 4 Hz. The system can run for long periods unattended, and a minimum of 300,000 FIDs were averaged for each 1 GHz portion, with some overnight runs providing in excess of 700,000 averaged FIDs. Due to system overhead requirements, the summary FID contains only 499,994 points (140 ps short of the full 10 μs). This is treated with a Kaiser-Bessel windowing function with a damping factor of 9.5 and zero-filled to a 2,097,152-point record length before Fourier transformation to the frequency domain with a resolution element of 23.84 kHz. As a result of the windowing, which reduces the $\sin x/x$ ringing in the frequency domain spectrum at the expense of broader lines, the observed line widths (FWHM) are approximately 225 kHz. The Balle-Flygare spectrometer has also been described previously.^{17,18} The time domain signal, after being down-converted twice by a two-stage heterodyne detection system to a center frequency of 2.5 MHz, is typically digitized for 1024

data points at a sampling frequency of 10 MHz and corrected for background. The background corrected signal is averaged and then zero filled to a 2048-point record length before Fourier transformation to give a frequency domain signal with a resolution element of 4.88 kHz. To resolve the deuterium quadrupole hyperfine components in the HCCD-containing isotopologues, twice as many points are digitized and zero-filled, giving a resolution element of 2.44 kHz. Since the molecular beam is parallel to the mirror axis in the cavity spectrometer, each transition appears as a Doppler doublet. The rest frequency of the transition is the mean frequency of the two Doppler components.

4. Results

4.1 Spectral analysis

Only *b* type transitions are observed in the chirped pulse spectrum for the ^{35}Cl - and ^{37}Cl -containing isotopologues of vinyl chloride-HCCH. These transitions are split by the nuclear quadrupole coupling interactions caused by the chlorine nucleus (both ^{35}Cl and ^{37}Cl have $I = 3/2$). The splitting pattern, combined with the relative abundances of the ^{35}Cl and ^{37}Cl isotopes, makes spectral assignment relatively simple. A sample pattern of these splittings is shown in Fig. 5 for the $2_{12} - 1_{01}$ transition for both the most abundant and ^{37}Cl -containing isotopologues.

Each chlorine hyperfine component for the eight isotopologues not containing deuterium appears simply as a Doppler doublet in the Balle-Flygare spectra. For the two HCCD-containing isotopologues, the chlorine hyperfine components are further split by the quadrupolar deuterium nucleus, an example of this is shown in Fig. 6 for a ^{35}Cl hyperfine component ($F_1 = 5/2 - 3/2$) of the $2_{12} - 1_{01}$ transition. Despite being weak, the more sensitive cavity spectrometer allows the observation of *a*-type transitions for most of the isotopologues, with the exception of species

containing ^{13}C in natural abundance and those containing HCCD, as transitions in these latter isotopologues exhibit extensive hyperfine splitting.

The spectrum for each isotopologue is analyzed using the Watson A -reduced Hamiltonian in the I' representation¹⁹ with the inclusion of chlorine nuclear quadrupole coupling interactions and, when appropriate, deuterium nuclear quadrupole coupling interactions. The angular momentum coupling scheme employed couples the rotational angular momentum of the complex (J) to the spin angular momentum of the chlorine nucleus (I_{Cl}) to give either the total angular momentum (F) for spectral lines that are not further split by a deuterium quadrupole interaction, or the intermediate angular momentum (F_1) for lines that are. In the latter case, F_1 couples to the spin angular momentum of deuterium (I_{D}), giving the total angular momentum. Using Pickett's nonlinear least squares computer program, SPFIT,²⁰ we fit, for each isotopologue, 3 rotational constants, 5 quartic centrifugal distortion constants, chlorine nuclear quadrupole coupling constants, and deuterium nuclear quadrupolar coupling constants for the HCCD-containing species. The values of these spectroscopic constants, together with the numbers and types of transitions analyzed, are listed in Table 2 for the two spectra obtained in the broadband, chirped pulse spectrometer, and in Tables 3, 4 and 5, for those obtained using the higher resolution, Balle-Flygare spectrometer. In addition, tables of observed and calculated transition frequencies with assignments for all isotopologues studied are available as supplementary material. The rms deviation of each fit is less than 11 kHz for the broadband data and is about 2 kHz for the narrow band data, representing a fraction of a typical line width in the respective technique.

The spectroscopic constants for the most abundant and ^{37}Cl -containing isotopologues derived from the broadband and narrow band spectrometers agree very well. We will use the constants from the latter technique exclusively in the following sections.

4.2 Structure determination

The values of the asymmetry parameters of the isotopologues of vinyl chloride-HCCH are between -0.87 and -0.85 and those of the inertial defect are between 0.29 and 0.32 amu \AA^2 , respectively. These values are consistent with an asymmetric planar complex where in-plane vibrational motions make the dominant contribution to the inertial defect. The experimentally determined rotational constants for the most abundant isotopologue differ from those predicted by theory for the top and side binding structures by $3.0\% - 4.9\%$ and $1.0\% - 2.5\%$, respectively. Thus, the agreement with the side binding configuration is best, but because we are comparing the rotational constants corresponding to the experimental, average structure with those corresponding to theoretical, equilibrium structures, the closer agreement does not rule out completely the top binding configuration as the observed structure.

Since five of the isotopologues, that with ^{37}Cl and those containing a single ^{13}C , each contain a single substitution in a heavy atom of $\text{CH}_2\text{CH}^{35}\text{Cl-HCCH}$, the absolute values of the substitution coordinates for these atoms (with respect to the principal axis system of the parent species) can be determined using a Kraitchman analysis²¹ (Table 6). The signs of these coordinates are determined separately as described below. The Kraitchman method assumes isotope independent vibration-rotation interactions, and the validity of this assumption increases with the distance of a substituted atom from an inertial plane. It is possible to show that a good, operational definition of the uncertainty in a substitution coordinate, r , is given by the so-called Costain error, which is $\sigma(r) = 0.0015 \text{\AA}^2/|r|$.²² Values of the Costain error for each substitution coordinate are given in Table 6.

The relative signs for the coordinates of the two C atoms and the Cl atom in vinyl chloride can be easily determined using the known values of its bond lengths (1.333\AA for C=C and 1.726\AA

for C-Cl).¹⁴ If we place the C atom bonded to Cl and H (C-1) in the first quadrant, then C-2 (the atom bonded to two H atoms) and Cl must be in the first and fourth quadrants, respectively, giving a C=C bond length of 1.321 Å and a C-Cl bond length of 1.731 Å. To satisfy the center-of-mass condition, the *a* coordinates of the C atoms in HCCH (C-3 and C-4) must be negative. Aside from a remaining ambiguity in the signs for the *b* coordinates of the carbon atoms in the acetylene molecule, this locates all the heavy atoms, and the hydrogen atoms can be placed using the known (and assumed unchanged) geometries of the monomers. The two possible signs for the *b* coordinates of the acetylenic carbons atoms, however, give two different orientations for HCCH (Fig. 7), but both of these orientations definitively places HCCH at one end of the C=C bond, not across. One of these two configurations (Fig. 7b) requires one of the H atoms in HCCH to be about 1.8 Å from the H atom bonded to C-1 of vinyl chloride, a distance that is shorter than the sum of the van der waals radii of two H atoms. Additionally, there are no other possible interactions between the subunits. Therefore, this structure can be eliminated. Consequently, we arrive at the configuration (Fig. 7a) that is seen to agree with the theoretical structure corresponding to the global minimum.

Using the singly substituted HCCD isotopologue, we have also calculated the Kraitchman coordinate for the substituted H atom (Table 6). Because the zero point motions for HCCH and HCCD may be significantly different, this set of coordinates is not as reliable for locating the substituted H atom as it is for heavier atoms. Nevertheless, using the only possible substitution structure, the signs for the coordinates can be easily determined, and the position of this atom serves to show that the observed HCCD isotopologue is one with D bound to the Cl atom. This substitution coordinate for D also provides a C-H bond length reasonably close (0.94703 Å) to that known for HCCH (1.05756 Å).¹⁵ The species with H participating in the hydrogen bond is

not observed, presumably because it is of higher energy and not populated in the cold jet expansion.

With the substitution structure, we proceed to determine more precisely the geometric parameters of the complex by fitting them to two independent moments of inertia for each of the ten isotopologues. We select I_a and I_c as the former is typically sensitive to the angular orientation of the subunits in a complex, and the latter to intermolecular distance. We use Schwendeman's STRFTQ program²³ and make the usual assumption that the structures of vinyl chloride¹⁴ and HCCH¹⁵ remain unchanged upon complexation. Different combinations of a distance between the two subunits and two angles that describe the orientations of the subunits are used to minimize correlations, and in the end, we use the following set of parameters: the length of a line connecting C-4 (see Fig. 7a) and the center of the C=C bond, and the angles that HCCH and C=C, respectively, make with this line. The greatest correlations are between the two angles (-0.96), otherwise there is little correlation between the distance and each of the two angles (-0.31 between the distance and the angle formed with C=C, and 0.55 between the distance and the angle formed with HCCH). The rms deviation of the fit is $0.0781 \text{ amu } \text{\AA}^2$. The resulting structure, reported with chemically relevant geometric parameters, is shown in Fig. 8a. Specifically, the CCl...H angle is $88.67(22)^\circ$, the hydrogen bond has a length of $3.014(14) \text{ \AA}$ and bends from linearity by $58.49(54)^\circ$. The length of the interaction between H geminal to Cl and the center of the C \equiv C bond is $2.9392(41) \text{ \AA}$. The coordinates of the atoms with a single substitution are listed in Table 5; they agree very well with the Kraitchman coordinates, although as expected, the agreement is not quite as good for the substitution of D for H in HCCH. It is worth noting that the uncertainties in the geometric parameters are indications of the zero point motions of the isotopologues. Since HCCH and HCCD may have very different zero point

motions, we considered also a fit in which the HCCD isotopologues were eliminated, but the correlation between the angles worsens and the uncertainties of the parameters do not improve significantly.

4.3 Quadrupole coupling constants

Of the four nonzero components of the chlorine quadrupole coupling tensor for each of the ten isotopologues, we have determined the three diagonal components (χ_{aa} , χ_{bb} , and χ_{cc}) and the magnitude of the only nonvanishing off-diagonal component, χ_{ab} . (χ_{bc} , and χ_{ac} are zero as a consequence of the planar structure of the complex.) Diagonalization of the tensor for the most abundant species yield the nuclear quadrupole coupling constants in the principal electric field gradient axis system, x, y, z , with the values of χ_{xx} , χ_{yy} , and χ_{zz} determined to be 31.3860 MHz, 37.0997 MHz, and -68.4857 MHz, respectively. The y and z axes are in the molecular plane, with the z axis taken to be that of the quadrupole coupling constant of the greatest magnitude. (Since the x axis is the same as the c axis, $\chi_{xx} = \chi_{cc}$.) The absolute value of the asymmetry parameter for the quadrupole coupling constants, $|\eta| = \left| (\chi_{xx} - \chi_{yy}) / \chi_{zz} \right|$, is 0.083 indicating that there is only a very small deviation from a cylindrical charge distribution about the z electric field gradient axis, which typically lies more or less along the C-Cl bond. Taking the C-Cl axis to be the z -axis, it makes an angle of 83.47° with the a axis of the complex, which agrees with the value of 84.01° derived from the structure fit.

The sign of χ_{ab} in the inertial axis system shown in Fig. 7a can be determined by the relation between the quadrupole coupling tensors of $\text{CH}_2\text{CH}^{35}\text{Cl-HCCH}$ and the $\text{CH}_2\text{CH}^{35}\text{Cl}$ monomer. Making the usual assumption that intermolecular interactions do not perturb the electric field gradient by a significant amount, that is, HCCH does not cause a noticeable

perturbation in the electronic arrangement about the chlorine nucleus, the nuclear quadrupole coupling tensors for vinyl chloride and for its HCCH complex are related by a rotation of the a and b inertial axes. The rotation matrix is simply the eigenvector matrix for the moment of inertia tensor of the dimer expressed in the monomer principal inertial axis system. This assumption is supported by *ab initio* calculation of the quadrupole coupling tensors for the two species using Gaussian 09¹³ at the MP2/6-311++G(2d, 2p) level and comparing the values of χ_{cc} , which are unaffected by the rotation about the c axis that connects the inertial axis systems of the monomer and the complex. For $\text{CH}_2\text{CH}^{35}\text{Cl}$, theory predicts $\chi_{cc} = 29.07$ MHz while for $\text{CH}_2\text{CH}^{35}\text{Cl-HCCH}$ $\chi_{cc} = 28.96$ MHz is obtained. Similarly, the experimental values for χ_{cc} are 31.74 MHz¹⁴ and 31.89 MHz for the monomer and complex, respectively. These differences of less than 0.4% can be taken to indicate a vanishingly small effect on the field gradient due to the presence of HCCH in the complex.

The best agreement with the experimental values of the quadrupole coupling constants for both the monomer and the dimer is obtained when the value of χ_{ab} for $\text{CH}_2\text{CH}^{35}\text{Cl-HCCH}$ is positive. Further confirmation of the sign of χ_{ab} is achieved by rotating the quadrupole tensor of the most abundant species of the complex in the same manner as the inertial tensor into each of the ^{35}Cl -containing isotopologues. A positive sign of χ_{ab} reproduces the experimentally determined quadrupole tensor for each of these complexes well. Both the rotation matrices and the calculated quadrupole coupling constants are available as supplementary material. The rotation of the quadrupole coupling tensor of $\text{CH}_2\text{CH}^{35}\text{Cl-HCCH}$ back into $\text{CH}_2\text{CH}^{35}\text{Cl}$ also yields an estimate of the value for the previously undetermined χ_{ab} of -34.7 MHz of $\text{CH}_2\text{CH}^{35}\text{Cl}$. Finally, a similar analysis also establishes the sign of χ_{ab} for $\text{CH}_2\text{CH}^{37}\text{Cl-HCCH}$.

Subsequently, by rotating the quadrupolar tensors of $\text{CH}_2\text{CH}^{35}\text{Cl}-\text{HCCH}$ and $\text{CH}_2\text{CH}^{37}\text{Cl}-\text{HCCH}$, respectively, into other ^{35}Cl and ^{37}Cl containing species, we are able to establish the signs for the χ_{ab} values for all isotopologues studied.

Although DCCH is close to the magic angle, so that χ_{aa} is not well-determined and its inclusion makes very little difference in the fit for $\text{CH}_2\text{CH}^{35}\text{Cl}-\text{DCCH}$, the deuterium nuclear quadrupole coupling constants also reveal geometric information. Once again, if there is no electric field gradient perturbation due to complexation, the deuterium quadrupole coupling constant, χ_{aa} , in the complex is simply a $\langle P_2 \rangle$ projection of the coupling constant in the HCCD monomer, 204.4(10) kHz. [The deuterium nuclear quadrupole coupling constant for DCCD has been measured to be 204.4(10) kHz²⁴ while that for HCCD is 200(10) kHz.²⁵ Since the two values should be similar, we use the more recent and more precise value here.] This relation gives an angle of 53.12(34)° between HCCD and the *a* axis of the dimer, which agrees well with the value of 53.83° obtained from the structure fit.

5. Discussion

The experimental average structure of vinyl chloride-HCCH (Fig. 8a) is very similar to the theoretical structure at the global minimum (Fig. 4b). Specifically, the interaction lengths are slightly longer in the average structure, by 0.029 Å for the hydrogen bond and by 0.105 Å for the H...acetylenic bond while the CCl...H angle is 2.17° greater. The deviations from linearity agree to approximately experimental uncertainty. The side bonding motif of the complex is different from that of its HF counterpart¹² (Fig. 2a), which is not the case for the fluoroethylene-containing complexes where the binding modes for HF, HCl, and HCCH are the same for a given fluoroethylene subunit. Despite this difference, the general trends are observed. The weaker acid HCCH forms a significantly longer hydrogen bond with vinyl chloride than HF (by 0.70 Å)

and bends by 39° more from linearity. The hydrogen bond involving HCCH is thus weaker. To understand the different binding modes, we map the electrostatic potential of vinyl chloride onto its total electron density surface (Fig. 9a), calculated at the MP2/6-311++ G (2*d*, 2*p*) level. The blue represents positive electrostatic potential and red negative electrostatic potential. Of the three hydrogen atoms, the one geminal to Cl is the most positive, it should, therefore, form the most favorable interaction with the nucleophilic portion of a protic acid. This is indeed observed in vinyl chloride-HCCH. If the F atom in HF were to interact with the most electropositive hydrogen atom in vinyl chloride with the same hydrogen bond length and secondary interaction length (H...FH) as observed experimentally in the top binding configuration, and with the CCl...H angle the same as found for vinyl chloride-HCCH in the side bonding configuration (88.67°), then the hydrogen bond in this putative side-binding HF complex would have to bend by 35° , which is 20° greater than is observed in the top binding configuration. We can therefore conclude that the distortion required to achieve a side-binding structure is too great, and the decrease in stability too much, for HF to bind at one end of the C=C bond.

The effect of halogen substitution can be examined by comparing vinyl chloride-HCCH (Fig. 8a) with vinyl fluoride-HCCH⁸ (Fig. 8b) and the mapped electrostatic potentials of vinyl chloride (Fig. 9a) with vinyl fluoride (Fig. 9b). It is apparent that F is much more electronegative than Cl; thus, it should form a much stronger hydrogen bond with HCCH, as supported by the fact that the bond is 0.57 \AA shorter and its deviation from linearity is 22° less in vinyl fluoride-HCCH as compared to vinyl chloride-HCCH. The much stronger hydrogen bond in vinyl fluoride-HCCH makes the interaction between the acetylenic bond and hydrogen of vinyl fluoride less important in stabilizing the complex. Thus, $\text{C}\equiv\text{C}$ interacts with an H atom that

is less positive than that geminal to F, but in doing so, avoids the steric strain that accompanies a side binding configuration.

It is interesting to note that the most negative potential in vinyl chloride is concentrated on a band centered about the chlorine atom and approximately perpendicular to the C-Cl bond while that in vinyl fluoride points away from the fluorine atom along the C-F bond. This suggests that for a certain binding mode, the angles CCl...H and CF...H reflect the direction of the electron density, and thus, the former angle is necessarily smaller. For vinyl chloride, the difference between the values of the CCl...H angles in the top and side binding modes also serves to reflect the manner in which the electron density is distributed about the Cl atom, as is also the case for the analogous CF...H angles in vinyl fluoride.

6. Conclusions

We have determined the structure of the gas-phase bimolecular complex formed between vinyl chloride and acetylene. Unlike the corresponding complex formed between vinyl chloride and hydrogen fluoride, which adopts a top binding configuration, the HCCH molecule binds at one end of the vinyl chloride and interacts with the chlorine atom and a hydrogen atom attached to the same carbon (C-1). This represents the first case for which we have observed different binding motifs in complexes containing the same haloethylene but a different protic acid. Specifically, one of the two hydrogen atoms in HCCH forms a hydrogen bond with the chlorine atom of vinyl chloride with a Cl...H distance of 3.01 Å and a CCl...H angle of 88.7°. The deviation of the hydrogen bond from linearity is 58.5°. The secondary interaction formed between the C≡C triple bond and the hydrogen atom geminal to the chlorine atom, being 2.939 Å long, is actually shorter than what we have been calling the hydrogen bond.

Nevertheless, the general trends of bonding in these haloethylene-protic acid complexes are still observed to hold. The weaker gas-phase acid acetylene forms a longer hydrogen bond in its complex with vinyl chloride than does the stronger gas-phase acid HF in its complex, and similarly displays a greater deviation from linearity.¹² Indeed, it is this difference in hydrogen bond interaction strength that is likely responsible for the observed change in binding motif. The steric requirements necessary to create a favorable secondary interaction with HF and HCCH are quite different. Achieving a more favorable secondary interaction for vinyl chloride-HF in a side binding configuration, analogous to that observed for vinyl chloride-HCCH, would require too much distortion in the stronger hydrogen bond interaction with HF, thereby weakening the bond to an unacceptable extent. Similarly in the vinyl fluoride-HCCH complex, a stronger hydrogen bond is favored over the secondary interaction strength. On the other hand, in vinyl chloride-HCCH, the hydrogen bond is less important to the stability of this complex and the (perhaps no longer appropriately named) secondary interaction is optimized instead.

The electron distribution surrounding the chlorine atom, which results in a concentration of negative electrostatic potential being concentrated in a band centered on the atom and approximately perpendicular to the C-Cl bond, allows for a smaller CX...H angle than is possible for hydrogen bonds to fluorine atoms. This further relaxes the steric requirements for a closer approach of the nucleophilic portion of the acid to a hydrogen atom on the haloethylene. The information provided by this study and that of the vinyl chloride-HF complex¹² regarding the electrostatic and steric preferences for the bonding of protic acids to chlorine in substituted ethylenes will be essential in understanding the interplay among these factors that will govern the structures of species in which the ethylene contains both chlorine and fluorine substitutions.

Acknowledgements

This material is based on work supported by the National Science Foundation under Grant No. CHE-1111504.

Supporting Information Available: Tables of observed and calculated transition frequencies for all spectra for all isotopologues of vinyl chloride-HCCH that are reported in this study are available as supplementary material, as are the rotation matrices and calculated nuclear quadrupole coupling constants for all isotopologues that were used in the analysis to arrive at the sign of the sole non-zero off-diagonal element of the quadrupole coupling tensor. This material is available free of charge via the Internet at <http://pubs.acs.org>

Table 1. Structural parameters for fluoroethylene-HX complexes

	H...F (Å)	CH...F (°)	Deviation from linearity (°)	Secondary interaction length (Å) ^j
CH ₂ CHF–HF ^a	1.892(14)	121.4	18.7(15)	2.734
CH ₂ CHF–HCl ^b	2.123(1)	123.7(1)	18.3(1)	3.162
CH ₂ CHF–HCCH ^c	2.441(4)	122.6(4)	36.5(2)	3.159
CH ₂ CF ₂ –HF ^d	1.98833(44)	122.41	29.99	2.7825(3)
CH ₂ CF ₂ –HCl ^e	2.33094(36)	122.41	34.22	3.07619(30)
CH ₂ CF ₂ –HCCH ^f	2.646(11)	122.41(79)	53.25(24)	3.005(21)
CHFCF ₂ –HF ^g	2.020(41)	109.0(13)	41.6(51)	2.7522(40)
CHFCF ₂ –HCl ^h	2.3416(7)	109.720(39)	47.729(13)	3.0796(5)
CHFCF ₂ –HCCH ⁱ	2.748(15)	104.49(15)	69.24(67)	2.8694(9)

^aRef. 1

^bRef. 4; structure refitted in Ref. 5

^cRef. 8

^dRef. 2

^eRef. 6; structure refitted in Ref. 2

^fRef. 9

^gRef. 3

^hRef. 7

ⁱRef. 10

^jThe secondary interaction length refers to the distance between the nucleophilic portion of the acid, namely, F, Cl, or the center of the acetylenic bond for HF, HCl, and HCCH, respectively, and the nearest hydrogen atom in the fluoroethylene subunit.

Table 2. Spectroscopic constants (in MHz, unless as otherwise noted) for two isotopologues of vinyl chloride-HCCH obtained from the broadband, chirped pulse spectrometer. 1σ standard deviations in the parameters are given in parentheses.

	CH ₂ CH ³⁵ Cl- HCCH	CH ₂ CH ³⁷ Cl- HCCH
<i>A</i>	5679.6182(15)	5560.5716(28)
<i>B</i>	1523.02024(44)	1512.61931(91)
<i>C</i>	1200.10948(44)	1188.26263(80)
$\Delta_J / 10^{-3}$	3.9827(49)	3.886(11)
$\Delta_{JK} / 10^{-3}$	4.129(30)	5.059(87)
$\Delta_K / 10^{-3}$	27.38(33)	23.47(51)
$\delta_J / 10^{-3}$	0.9920(21)	0.9857(37)
$\delta_K / 10^{-3}$	16.838(95)	16.18(33)
χ_{aa} (Cl) ^a	35.7483(81)	28.021(14)
χ_{bb} (Cl) ^a	-67.1371(78)	-52.754(11)
χ_{cc} (Cl) ^a	31.3888(66)	24.733(11)
χ_{ab} (Cl) ^b	11.2(11)	10.16(27)
No. of rotational transitions	25	21
No. of <i>a</i> type transitions	0	0
No. of <i>b</i> type transitions	25	21
No. of hyperfine components	102	82
<i>J</i> range	0 – 7	0 – 7
<i>K_a</i> range	0 – 2	0 – 2
rms / kHz	7.40	10.29

^aThe nuclear quadrupole coupling constants of chlorine are fitted as $1.5 \chi_{aa}$ and $(\chi_{bb} - \chi_{cc})/4$, and the Laplace condition is used to calculate the individual hyperfine constants.

^bThe signs of both χ_{ab} values are determined to be positive. See Section 4.3 for details and the coordinate system used.

Table 3. Spectroscopic constants (in MHz, except as otherwise noted) for four isotopologues of vinyl chloride-acetylene formed with HCCH and H¹³C¹³CH. 1 σ standard deviations in the parameters are given in parentheses.

	CH ₂ CH ³⁵ Cl– HCCH	CH ₂ CH ³⁷ Cl– HCCH	CH ₂ CH ³⁵ Cl– H ¹³ C ¹³ CH	CH ₂ CH ³⁷ Cl– H ¹³ C ¹³ CH
<i>A</i>	5679.61727(14)	5560.57045(13)	5648.87874(15)	5531.54237(14)
<i>B</i>	1523.020752(58)	1512.619734(61)	1449.555412(63)	1438.905072(87)
<i>C</i>	1200.109280(46)	1188.262524(50)	1152.747245(54)	1141.061070(64)
$\Delta_J / 10^{-3}$	3.98225(55)	3.89434(60)	3.64080(58)	3.55789(88)
$\Delta_{JK} / 10^{-3}$	4.0807(40)	4.9268(40)	3.1586(45)	3.9472(58)
$\Delta_K / 10^{-3}$	27.066(14)	23.208(14)	28.362(15)	24.549(14)
$\delta_J / 10^{-3}$	0.99201(32)	0.97624(33)	0.87931(34)	0.86346(64)
$\delta_K / 10^{-3}$	17.041(14)	16.797(15)	15.788(17)	15.586(23)
χ_{aa} (Cl) ^a	35.73569(81)	28.00512(83)	35.64180(93)	27.92631(95)
χ_{bb} (Cl) ^a	−67.12170(97)	−52.74184(94)	−67.0273(11)	−52.6638(11)
χ_{cc} (Cl) ^a	31.38602(89)	24.73672(90)	31.3855(10)	24.7375(10)
χ_{ab} (Cl) ^b	11.92(11)	9.987(24)	11.84(22)	9.93(23)
No. of rotational transitions	60	48	60	47
No. of <i>a</i> type transitions	22	11	23	15
No. of <i>b</i> type transitions	38	37	37	32
No. of hyperfine components	365	264	322	236
<i>J</i> range	0 – 8	0 – 8	0 – 8	0 – 8

K_a range	0 – 3	0 – 3	0 – 3	0 – 3
rms / kHz	1.90	1.63	1.94	1.66

^aThe nuclear quadrupole coupling constants of chlorine are fitted as $1.5 \chi_{aa}$ and $(\chi_{bb} - \chi_{cc})/4$, and the Laplace condition is used to calculate the individual hyperfine constants.

^bThe signs of all χ_{ab} values are determined to be positive. See Section 4.3 for details and the coordinate system used.

Table 4. Spectroscopic constants (in MHz, except as otherwise noted) for four naturally occurring ^{13}C isotopologues of vinyl chloride-HCCH. 1σ standard deviations in the parameters are given in parentheses.

	$\text{CH}_2^{13}\text{CH}^{35}\text{Cl}-$ HCCH	$^{13}\text{CH}_2\text{CH}^{35}\text{Cl}-$ HCCH	$\text{CH}_2\text{CH}^{35}\text{Cl}-$ H^{13}CCH	$\text{CH}_2\text{CH}^{35}\text{Cl}-$ HC^{13}CH
A	5646.48124(80)	5531.4874(11)	5670.52513(72)	5659.1374(11)
B	1519.55812(52)	1506.67077(69)	1493.94201(31)	1476.05143(75)
C	1196.49929(58)	1183.25866(75)	1181.59744(33)	1169.87020(82)
$\Delta_J / 10^{-3}$	3.9850(56)	3.8915(76)	3.7846(32)	3.8211(65)
$\Delta_{JK} / 10^{-3}$	4.036(38)	3.463(52)	3.926(33)	3.521(69)
$\Delta_K / 10^{-3}$	25.84(15)	27.65(19)	27.94(14)	26.91(21)
$\delta_J / 10^{-3}$	0.9959(25)	0.9827(33)	0.9323(21)	0.9391(26)
$\delta_K / 10^{-3}$	17.39(30)	16.60(40)	16.57(17)	15.74(41)
$\chi_{aa}(\text{Cl})^a$	35.8132(26)	36.0248(41)	35.8293(23)	35.5543(53)
$\chi_{bb}(\text{Cl})^a$	-67.2168(22)	-67.3928(30)	-67.2158(21)	-66.9396(26)
$\chi_{cc}(\text{Cl})^a$	31.4036(26)	31.3680(40)	31.3864(23)	31.3852(55)
$\chi_{ab}(\text{Cl})^b$	11.72(27)	10.545(44)	11.32(46)	12.23(52)
No. of rotational transitions	18	19	20	17
No. of a type transitions	0	0	0	0
No. of b type transitions	18	19	20	17
No. of hyperfine components	60	61	70	48
J range	0 – 7	0 – 7	0 – 7	0 – 7

K_a range	0 – 2	0 – 2	0 – 2	0 – 2
rms / kHz	1.78	2.43	1.77	1.84

^aThe nuclear quadrupole coupling constants of chlorine are fitted as $1.5 \chi_{aa}$ and $(\chi_{bb} - \chi_{cc})/4$, and the Laplace condition is used to calculate the individual hyperfine constants.

^bThe signs of all χ_{ab} values are determined to be positive. See Section 4.3 for details and the coordinate system used.

Table 5. Spectroscopic constants (in MHz, except as otherwise noted) for two isotopologues of vinyl chloride-DCCH. 1σ standard deviations in the parameters are given in parentheses.

	CH ₂ CH ³⁵ Cl- DCCH	CH ₂ CH ³⁷ Cl- DCCH
<i>A</i>	5598.18981(45)	5483.33279(55)
<i>B</i>	1504.99128(15)	1494.60538(26)
<i>C</i>	1185.32439(13)	1173.66568(21)
$\Delta_J / 10^{-3}$	3.7673(18)	3.6826(35)
$\Delta_{JK} / 10^{-3}$	2.149(16)	2.987(20)
$\Delta_K / 10^{-3}$	32.916(83)	28.95(11)
$\delta_J / 10^{-3}$	0.9536(10)	0.9370(18)
$\delta_K / 10^{-3}$	15.894(65)	15.63(11)
χ_{aa} (Cl) ^a	35.9445(13)	28.1824(12)
χ_{bb} (Cl) ^a	-67.3405(13)	-52.9278(13)
χ_{cc} (Cl) ^a	31.3960(12)	24.7454(12)
χ_{ab} (Cl) ^b	10.69(20)	9.19(24)
χ_{aa} (D) ^a	0.0082(17)	0.0117(17)
χ_{bb} (D) ^a	0.0871(15)	0.0830(15)
χ_{cc} (D) ^a	-0.0953(15)	-0.0946(15)
No. of rotational transitions	22	18
No. of <i>a</i> type transitions	0	0
No. of <i>b</i> type transitions	22	18
No. of hyperfine components	272	199
<i>J</i> range	0 – 7	0 – 6
<i>K_a</i> range	0 – 2	0 – 2
rms / kHz	2.01	1.86

^aThe nuclear quadrupole coupling constants of chlorine and deuterium are fitted as $1.5 \chi_{aa}$ and $(\chi_{bb} - \chi_{cc})/4$ for each nucleus, and the Laplace condition is used to calculate the individual hyperfine constants.

^bThe signs of all χ_{ab} values are determined to be positive. See Section 4.3 for details and the coordinate system used.

Table 6. The coordinates of atoms with a single substitution in CH₂CHCl–HCCH.

	C-1	C-2	C-3	C-4	Cl	H ^a
(i) Substitution coordinates ^{b,c}						
<i>a</i> / Å	0.8721(17)	1.89583(79)	–2.55084(59)	–3.26031(46)	1.0767(14)	–1.99356(75)
<i>b</i> / Å	0.7266(21)	1.56128(96)	–0.3842(39)	0.5820(26)	–0.9923(15)	–1.1499(13)
(ii) From fit to moments of inertia						
<i>a</i> / Å	0.8893	1.9297	–2.5584	–3.2716	1.0695	–1.9342
<i>b</i> / Å	0.7210	1.5543	–0.3871	0.5883	–0.9956	–1.2408

^aThis is the hydrogen atom of acetylene that bonds to C-3 and that participates in the hydrogen bond.

^bCostain errors in the parameters are given in parentheses.

^cA Kraitchman analysis gives the absolute values of the substitution coordinates. The signs are derived from a consideration of known bond lengths.

References

1. Cole, G. C.; Legon, A. C. A characterisation of the complex vinyl fluoride•••hydrogen fluoride by rotational spectroscopy and ab initio calculations. *Chem. Phys. Lett.* **2004**, *400*, 419-424.
2. Leung, H. O.; Marshall, M. D.; Drake, T. L.; Pudlik, T.; Savji, N.; McCune, D. W. Fourier transform microwave spectroscopy and molecular structure of the 1,1-difluoroethylene–hydrogen fluoride complex. *J. Chem. Phys.* **2009**, *131*, 204301.
3. Leung, H. O.; Marshall, M. D. Rotational spectroscopy and molecular structure of 1,1,2-trifluoroethylene and the 1,1,2-trifluoroethylene-hydrogen fluoride complex. *J. Chem. Phys.* **2007**, *126*, 114310.
4. Kisiel, Z.; Fowler, P. W.; Legon, A. C. Rotational spectrum, structure, and chlorine nuclear quadrupole tensor of the vinyl fluoride-hydrogen chloride dimer. *J. Chem. Phys.* **1990**, *93*, 3054-3062.
5. Legon, A. C.; Ottaviani, P. A non-linear hydrogen bond F•••H-Br in vinyl fluoride•••HBr characterised by rotational spectroscopy. *Phys. Chem. Chem. Phys.* **2002**, *4*, 4103-4108.
6. Kisiel, Z.; Fowler, P. W.; Legon, A. C. Investigation of the rotational spectrum of the hydrogen-bonded dimer CF₂CH₂•••HCl. *J. Chem. Soc. Faraday Trans.* **1992**, *88*, 3385-3391.
7. Leung, H. O.; Marshall, M. D.; Ray, M. R.; Kang, J. T. Rotational spectroscopy and molecular structure of the 1,1,2-trifluoroethylene-hydrogen chloride complex. *J. Phys. Chem. A* **2010**, *114*, 10975-10980.

8. Cole, G. C.; Legon, A. C. Non-linearity of weak B ••• H-C hydrogen bonds: an investigation of a complex of vinyl fluoride and ethyne by rotational spectroscopy. *Chem. Phys. Lett.* **2003**, *369*, 31-40.
9. Leung, H. O.; Marshall, M. D. Rotational spectroscopy and molecular structure of the 1,1-difluoroethylene-acetylene complex. *J. Chem. Phys.* **2006**, *125*, 154301.
10. Leung, H. O.; Marshall, M. D.; Cashion, W. T.; Chen, V. L. Rotational spectroscopy and molecular structure of the 1,1,2-trifluoroethylene-acetylene complex. *J. Chem. Phys.* **2008**, *128*, 064315.
11. Leung, H. O.; Marshall, M. D.; Amberger, B. K. Fourier transform microwave spectroscopy and molecular structure of the *trans*-1,2-difluoroethylene–hydrogen fluoride complex. *J. Chem. Phys.* **2009**, *131*, 204302.
12. Leung, H. O.; Marshall, M. D.; Bozzi, A. T.; Cohen, P. M.; Lam, M.; Lee, A. J. Comparing the effects of fluorine and chlorine substitution on the intermolecular interactions in complexes between haloethylenes and hydrogen fluoride. *The 244th National Meeting of the American Chemical Society* **2012**, Division of Physical Chemistry, Paper 339, Philadelphia, Pennsylvania, 2012.
13. Frisch, M. J.; Trucks, G. W.; Schlegel, H. B.; Scuseria, G. E.; Robb, M. A.; Cheeseman, J. R.; Scalmani, G.; Barone, V.; Mennucci, B.; Petersson, G. A. et al. *Gaussian 09*, Revision B.01; Gaussian, Inc.: Wallingford, CT, 2009
14. Hayashi, M.; Inagusa, T. Microwave spectrum, structure and nuclear quadrupole coupling constant tensor of ethyl chloride and vinyl chloride. *J. Mol. Struct.* **1990**, *220*, 103-117.

15. Herman, M.; Campargue, A.; El Idrissi, M. I.; Vander Auwera, J. Vibrational spectroscopic database on acetylene $X^1\Sigma^{+g}$. *J. Phys. Chem. Ref. Data.* **2003**, *32*, 921-1360.
16. Marshall, M. D.; Leung, H. O.; Scheetz, B. Q.; Thaler, J. E.; Muentzer, J. S. A chirped pulse Fourier transform microwave study of the refrigerant alternative 2,3,3,3-tetrafluoropropene. *J. Mol. Spectrosc.* **2011**, *266*, 37-42.
17. Marshall, M. D.; Leung, H. O.; Calvert, C. E. Molecular structure of the argon-(Z)-1-chloro-2-fluoroethylene complex from chirped-pulse and narrow-band Fourier transform microwave spectroscopy. *J. Mol. Spectrosc.* **2012**, *280*, 97-103.
18. Leung, H. O.; Gangwani, D.; Grabow, J. U. Nuclear quadrupole hyperfine structure in the microwave spectrum of Ar-N₂O. *J. Mol. Spectrosc.* **1997**, *184*, 106-112.
19. Watson, J. K. G. Aspects of Quartic and Sextic Centrifugal Effects on Rotational Energy Levels. Durig, J. R., Ed.; Elsevier Scientific Publishing: Amsterdam, 1977; pp 1-89.
20. Pickett, H. M. The fitting and prediction of vibration-rotation spectra with spin interactions. *J. Mol. Spectrosc.* **1991**, *148*, 371-377.
21. Kraitchman, J. Determination of molecular structure from microwave spectroscopic data. *Am. J. Phys.* **1953**, *21*, 17-24.
22. Harmony, M. D.; Laurie, V. W.; Kuczkowski, R. L.; Schwendeman, R. H.; Ramsay, D. A.; Lovas, F. J.; Lafferty, W. J.; Maki, A. G. Molecular structures of gas-phase polyatomic molecules determined by spectroscopic methods. *J. Phys. Chem. Ref. Data.* **1979**, *8*, 619-721.

23. Schwendeman, R. H. In *Critical Evaluation of Chemical and Physical Structural Information*, Lide, D. R., Paul, M. A., Eds.; National Academy of Science: Washington, DC, 1974.
24. DeLeon, R. L.; Muentner, J. S. Structure and properties of the argon•acetylene van der Waals molecule. *J. Chem. Phys.* **1980**, *72*, 6020-6023.
25. Harrison, J. F. Nuclear quadrupole coupling constants in polyatomic molecules. *J. Chem. Phys.* **1968**, *48*, 2379-2380.

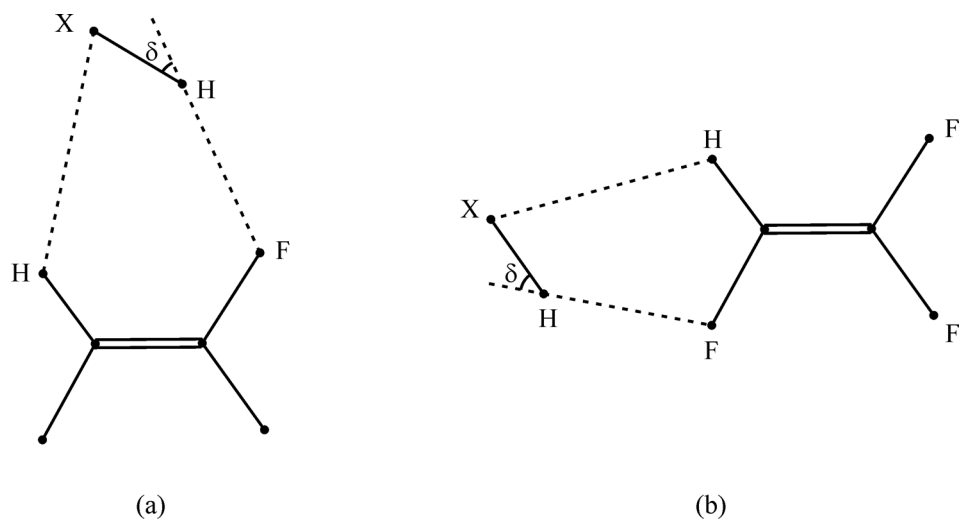


Figure 1. Examples of the two structure motifs observed in complexes formed between fluoroethylenes and protic acids. In the top binding configuration (a) as observed for complexes with vinyl fluoride and 1,1-difluoroethylene, the interactions between the subunits occur across the C=C bond, while in the side binding configuration (b), such as is found for complexes with 1,1,2-trifluoroethylene, the protic acid is at one end of the C=C bond.

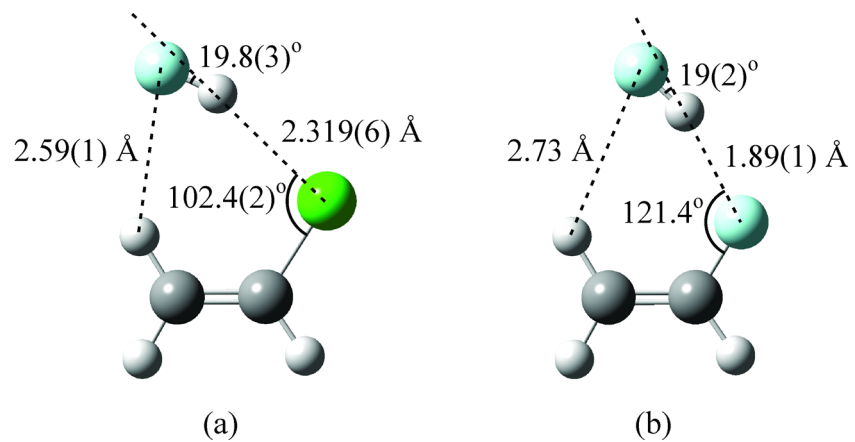


Figure 2. The similar top binding structures determined experimentally for (a) vinyl chloride-HF¹² and (b) vinyl fluoride-HF.¹ Note however, the smaller CCl...H angle and shorter secondary interaction in the vinyl chloride complex.

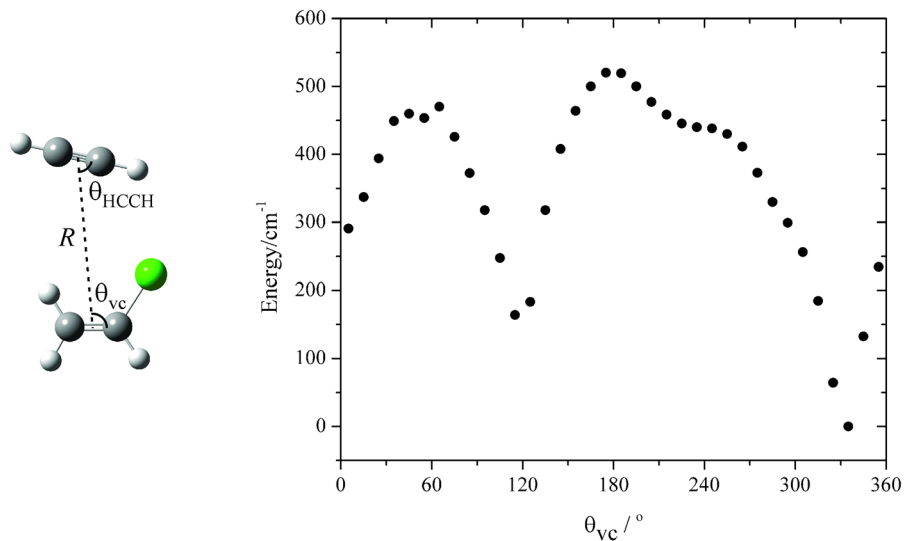


Figure 3. A relaxed scan of the MP2/6-311++G(2d, 2p) interaction potential between acetylene and vinyl chloride. The subunit geometries are held fixed at those of the free monomers, and only planar configurations of the complex are considered. The relevant structural parameters are shown in the inset. In the scan, the angular orientation of the vinyl chloride molecule (θ_{vc}) is varied from 5° to 355° in 10° steps, and the distance between the two subunits (R) and the orientation of the acetylene (θ_{HCCH}) are optimized at each step.

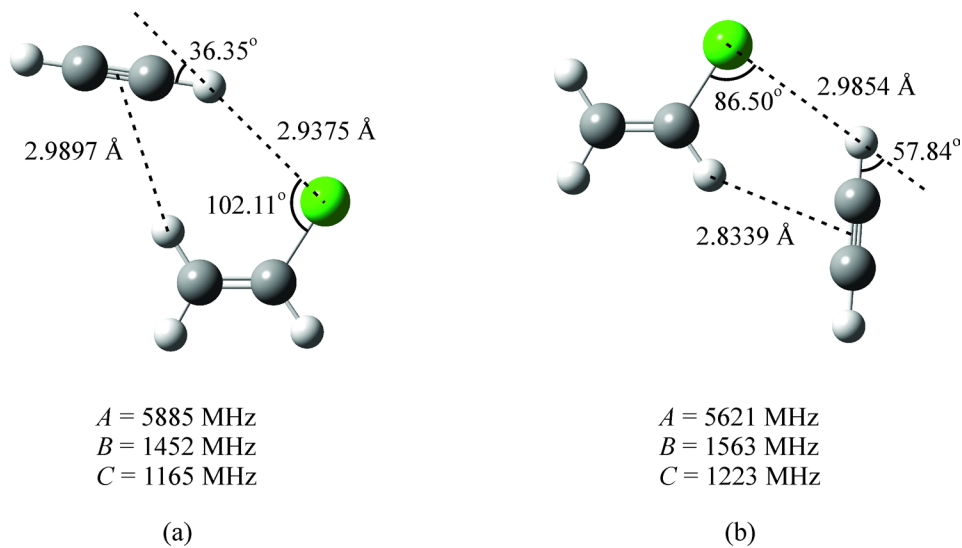


Figure 4. Optimized *ab initio* [MP2/6-311++G(2d, 2p)] geometries corresponding to the two structurally important minima displayed in the relaxed potential scan of Fig. 3 and the rotational constants predicted for these isomers. The top binding structure with $\theta_{vc} \approx 120^\circ$ is 152 cm^{-1} higher in energy than the side binding form with $\theta_{vc} \approx 340^\circ$.

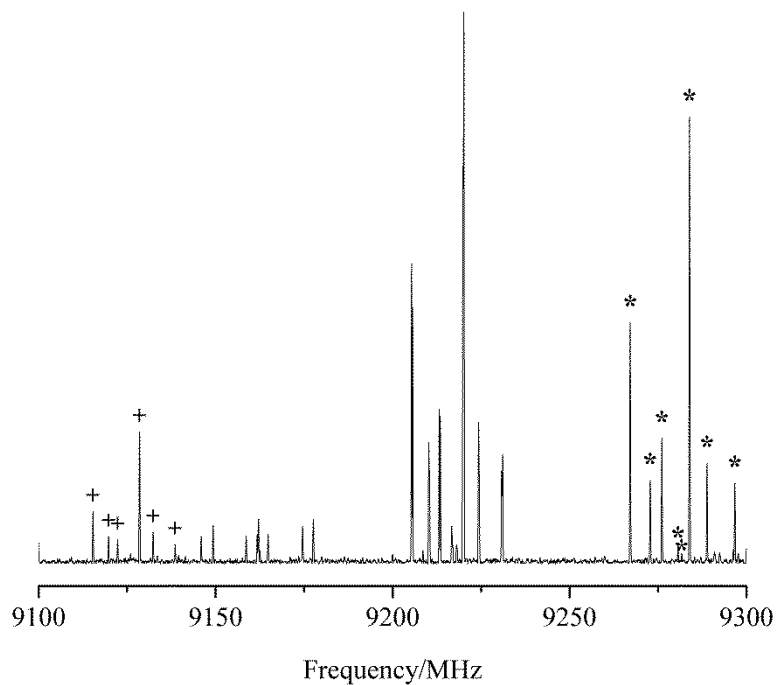


Figure 5. A 200 MHz portion of the broadband, chirped pulse Fourier transform microwave spectrum of vinyl chloride-HCCH, obtained as described in the text. Peaks marked with a “*” are due to the $2_{12} - 1_{01}$ rotational transition in $\text{CH}_2\text{CH}^{35}\text{Cl-HCCH}$ and those with a “+” are from the same transition in $\text{CH}_2\text{CH}^{37}\text{Cl-HCCH}$. The group of transitions at 9200 – 9230 MHz is due to argon-vinyl chloride, formed in the argon carrier gas jet expansion. The weaker peaks near 9150 – 9175 MHz are unassigned.

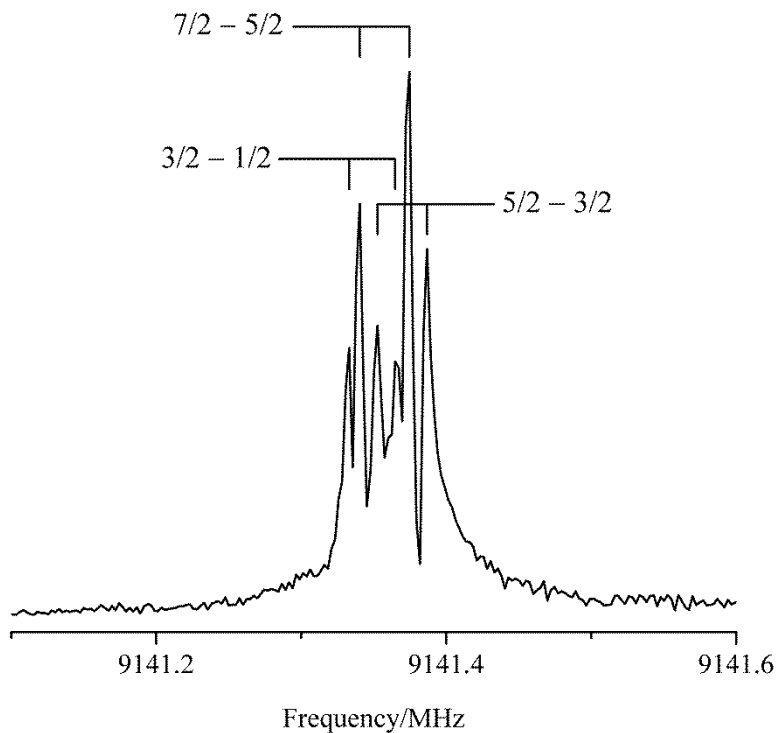


Figure 6. Splitting of the $F_1 = 5/2 - 3/2$ chlorine nuclear quadrupole hyperfine component of the $2_{12} - 1_{01}$ rotational transition in $\text{CH}_2\text{CH}^{35}\text{Cl}\text{-DCCH}$ due to the nuclear quadrupole coupling interaction of the deuterium nucleus. This spectrum was obtained using the narrow band, Balle-Flygare instrument described in the text, and each transition appears as a doublet, labeled by the corresponding F quantum numbers, due to the Doppler Effect.

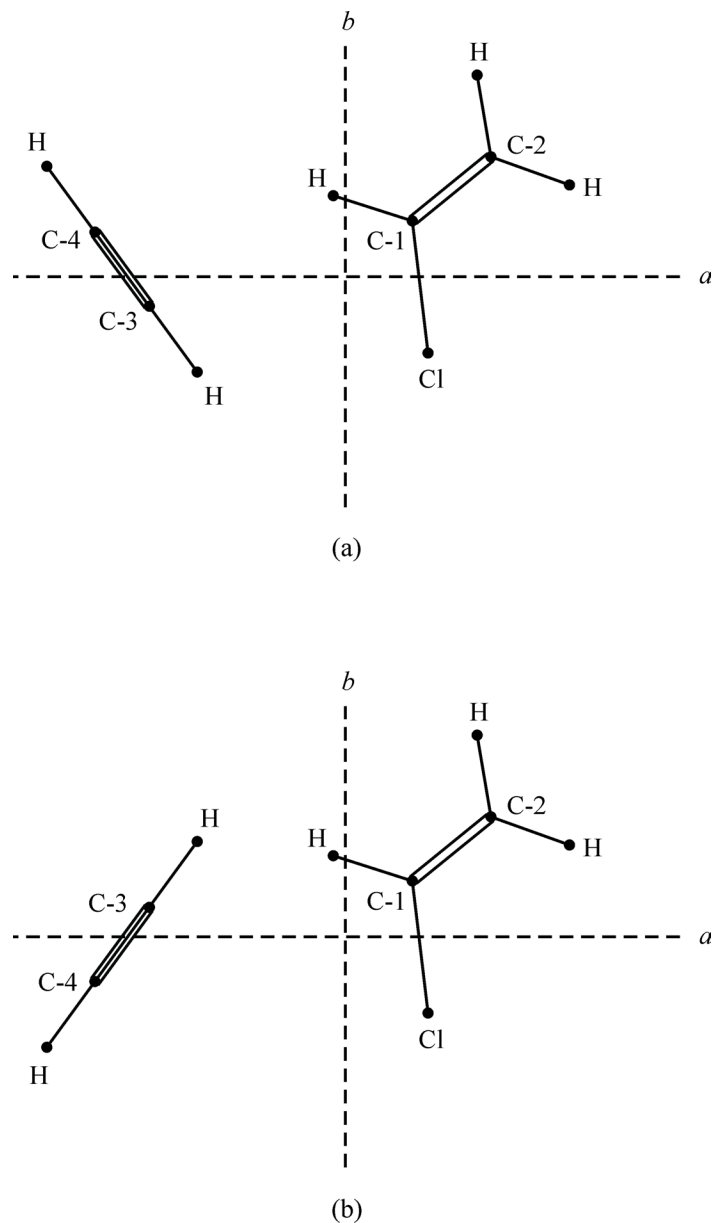


Figure 7. Two possible structures for the vinyl chloride-HCCH complex consistent with the substitution coordinates obtained using a Kraitchman analysis and known monomer geometries as described in the text. Both possibilities place the HCCH molecule at one end of the vinyl chloride in a side binding arrangement, but that shown in (b) would result in a H...H distance of 1.8 Å, which is much smaller than the sum of the van der Waals radii for two H atoms. Thus, (a) is the preferred structure.

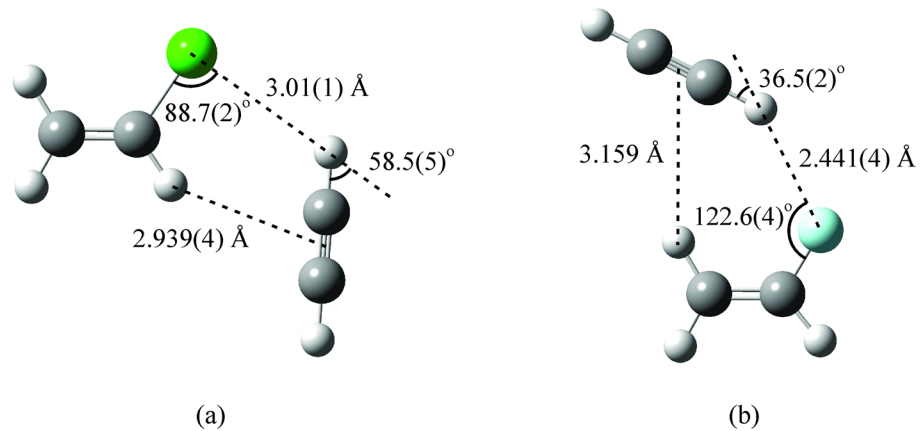


Figure 8. The experimentally determined structure (a) of vinyl chloride-HCCH determined from a fit to two independent moments of inertia for each of 10 isotopologues. Chemically relevant geometric parameters are indicated and compared with those for vinyl fluoride-HCCH, (b).⁸

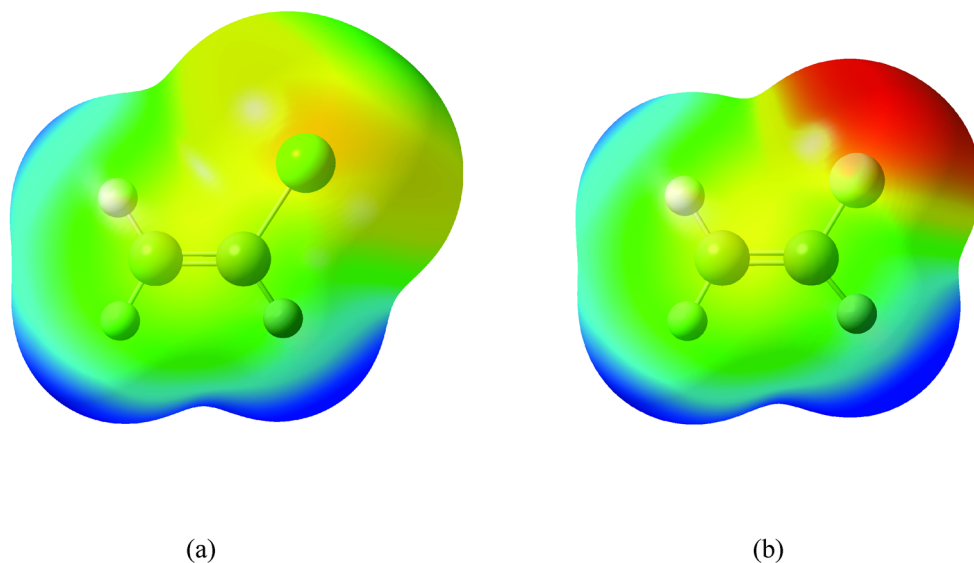
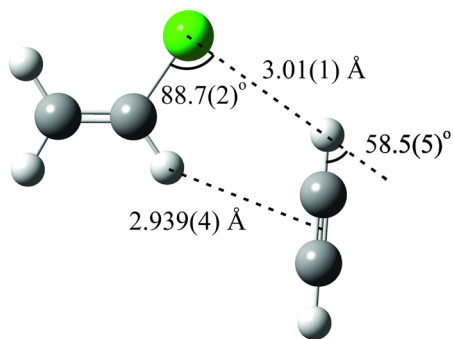
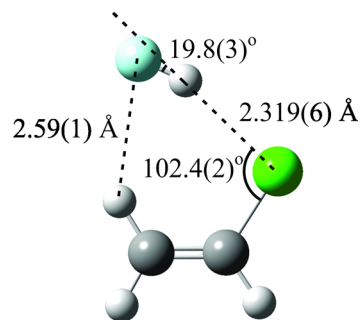


Figure 9. The electrostatic potential of (a) vinyl chloride and (b) vinyl fluoride mapped onto the respective electron density surfaces. Blue color represents positive electrostatic potential and red, negative electrostatic potential. In both molecules, the most positive H atom is the one geminal to the halogen atom. As expected, the F atom in vinyl fluoride is much more electronegative than is the Cl atom in vinyl chloride.

TOC Graphic



vinyl chloride-HCCH
side binding



vinyl chloride-HF
top binding